SAND2024-09179C

Pore-scale reactive transport and flow behavior involving dissolution and precipitation in heterogeneous porous media

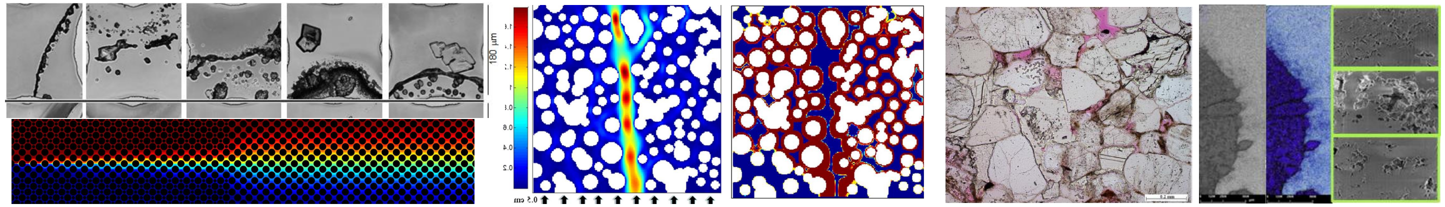

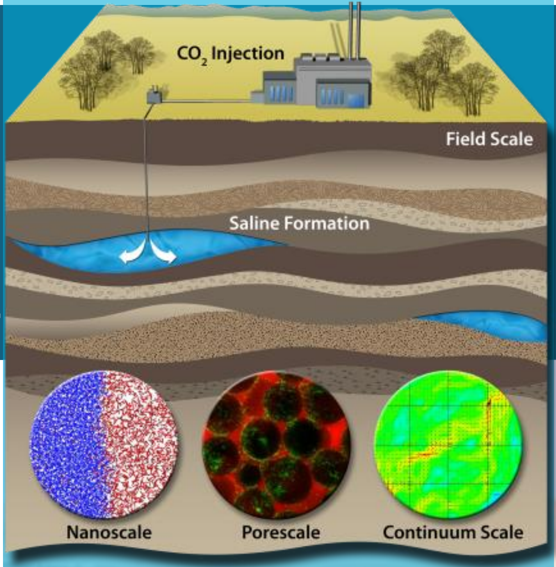

Hongkyu Yoon
Geoscience Research & Applications
Sandia National Laboratories, NM

WCCM, 2024, Vancouver, Canada

SAND2024-XXXXC

This work was supported by the U.S. Department of Energy, Office of Science Energy Earthshot Initiative, as part of the Advanced Multi-Physics Machine Learning for Subsurface Energy Systems Across Scales.

- **Motivations**
- **Reactive transport processes**
- Validation of pore scale transport models
- Precipitation and dissolution cases
- Other applications
- Summary

Motivations

- Fundamental understanding of pore scale reactive transport has been significantly improved over the past ~15+ years (e.g., RiMG 2015, 2019)
- Various studies on hydrodynamics, reactive transport, and coupled processes (e.g., chemo-mechanical coupling) are motivated with many subsurface applications (geologic carbon storage, unconventional resources recovery, nuclear waste repository, geothermal energy, etc.) and multiphysics in porous media (contaminant transport, fuel cells, flow& transport in varying saturated media, membrane filter systems, etc.)
- Both experimental and numerical capabilities have been improved with sensing and experimental apparatus and computational hardware & algorithms

Motivations

- Fundamental understanding of pore scale reactive transport has been significantly improved over the past ~15+ years (e.g., RiMG 2015, 2019)
- Various studies on hydrodynamics, reactive transport, and coupled processes (e.g., chemo-mechanical coupling) are motivated with many subsurface applications (geologic carbon storage, unconventional resources recovery, nuclear waste repository, geothermal energy, etc.) and multiphysics in porous media (contaminant transport, fuel cells, flow& transport in varying saturated media, membrane filter systems, etc.)
- Both experimental and numerical capabilities have been improved with sensing and experimental apparatus and computational hardware & algorithms
- A few new emerging techniques can be utilized to improve these continuing efforts
- One overarching question is what fundamental knowledge needs to be improved and how micro- and macro-processes are meaningfully integrated, depending on our scientific and practical interests

Reactive Transport Processes

- Multi-species in aqueous phase are transported by fluid(s) through advection and diffusion & react within aqueous phase (homogeneous reaction) and with the surface of the solids (heterogenous reactions - dissolution & precipitation)
- Reactive transport (RT) is represented by a mixed equilibrium and kinetic expression (aqueous speciation in equilibrium and kinetic reaction rates for dissolution/precipitation)

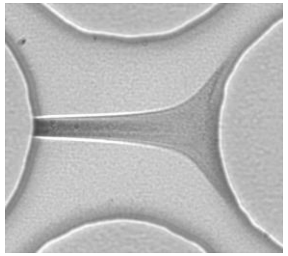

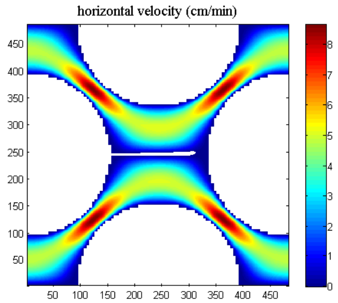

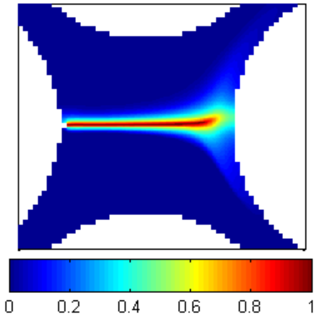

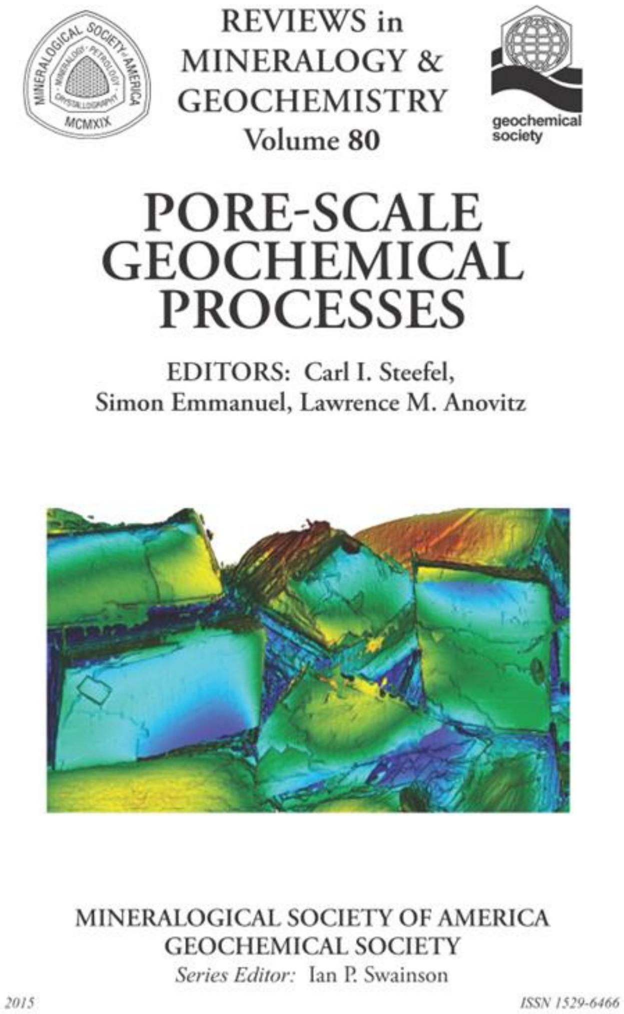

Pore Scale Reactive Transport Processes

- Multi-species in aqueous phase are transported by fluid(s) through advection and diffusion & react within aqueous phase (homogeneous reaction) and with the surface of the solids (heterogenous reactions - dissolution & precipitation)
- Reactive transport (RT) is represented by a mixed equilibrium and kinetic expression (aqueous speciation in equilibrium and kinetic reaction rates for dissolution/precipitation)
- Pore scale RT utilizes the geometry of phases and mineralogy at the resolution of interest
- Hydrodynamics for fluid flow is governed by the steady Stokes equation
- No solid phase movement, but change in the solid volume through reactions

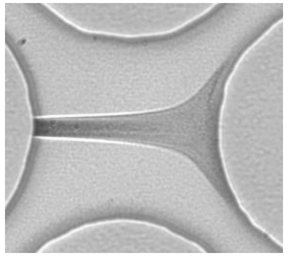

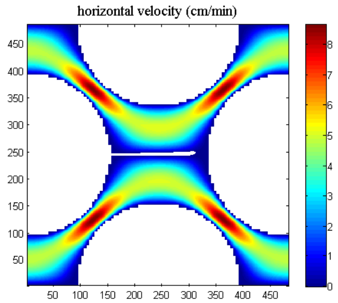

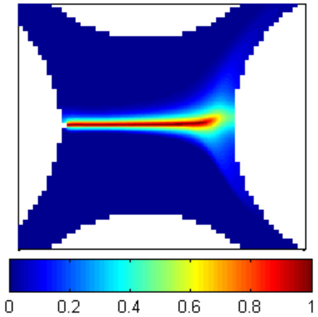

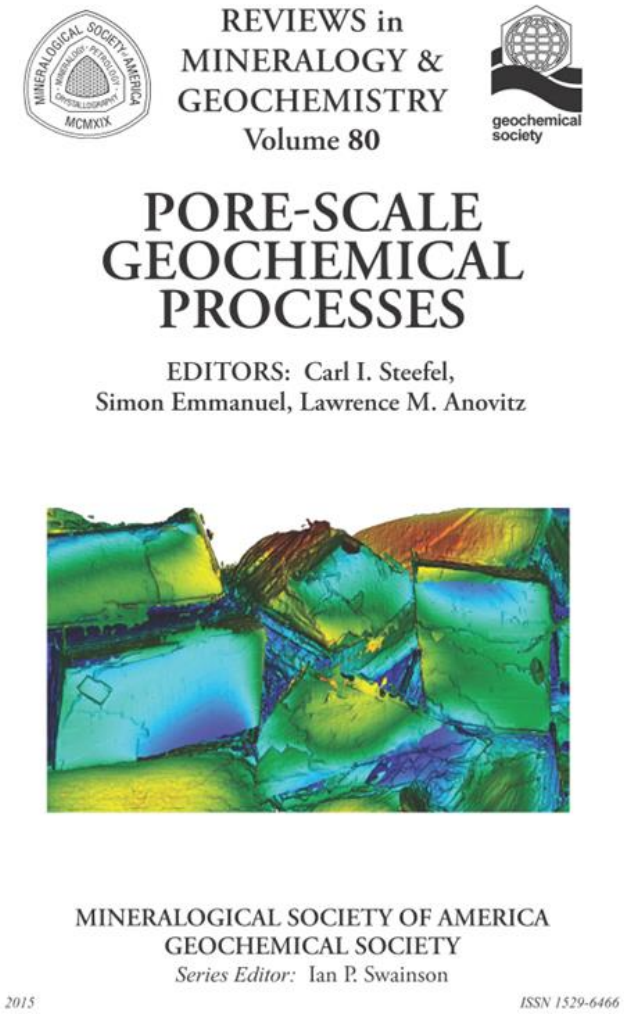

Pore scale modeling with precipitation and dissolution

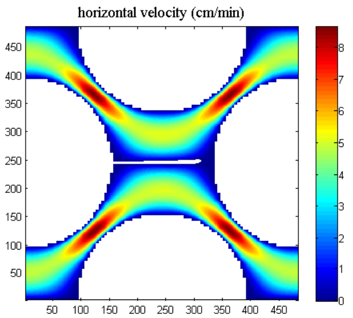

Navier-Stokes equation => Stokes equation with constant viscosity (independent of the species conc.) and at low Reynolds Re= ρ|**u**|*l* / μ«1

$$\nabla p = \mu \nabla^2 \mathbf{u} + \mathbf{F}$$

Step 1: Velocity field (u) at pore scale (Lattice Boltzmann Method)

Step 2: Reactive transport at pore scale (Finite Volume Method)

$$\frac{\partial \Psi_j}{\partial t} + (\mathbf{u} \cdot \nabla)\, \Psi_j - \nabla \cdot (D_j \nabla \Psi_j) = -\sum_{k=1}^{N_m} v_{jk} R_k + R_{\text{bio}}$$

Yoon et al. (RiMG, 2015)

Δt

$$\Psi_j = C_j + \sum_{i=1}^{N_{eq}} \upsilon_{ji} C_i$$

Chemical equilibrium in bulk fluid (e.g., H^+, HCO_3^-, …)
Extended Debye-Hückel Equation for activity coefficients

Phreeqc, GEMS

- Charge balance equation can be added
- Fracture aperture can be updated with mechanical coupling

$$D \frac{\partial \Psi_j}{\partial \mathbf{n}} = -I_m$$

on reactive surface (heterogeneous reaction)

$$I_m = -k_{cc}(1-\Omega) = -\left(k_1 a_{H^+} + k_2 a_{H_2CO_3} + k_3\right)\left(1 - \frac{Q_{cc}}{K_{sp}}\right)$$

Step 3: Update of $CaCO_3$ volumetric content (V_m)

$$\frac{\partial V_m}{\partial t} = \overline{V_m} s_m k_{cc} \left(\left[\frac{a_{Ca^{2+}} a_{CO_3^{2-}}}{K_{sp}} \right]^n - 1 \right)^m$$

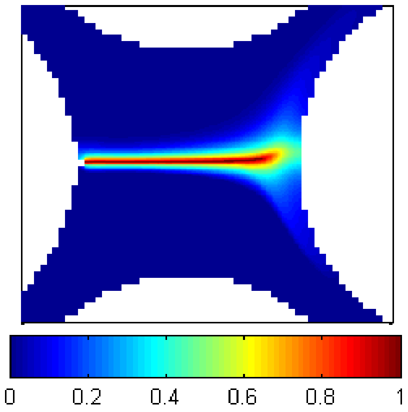

Crystal growth: Cellular automata algorithm

Volumetric $CaCO_3$ content

Zhang et al. (EST, 2010), Yoon et al. (WRR, 2012), Fanizza et al. (WRR, 2013), Boyd et al. (GCA, 2014), Singh et al. (EST, 2015), Yoon et al. (2015, 2017, EST 2019)

Crystal Growth and Dissolution at Pore Scale

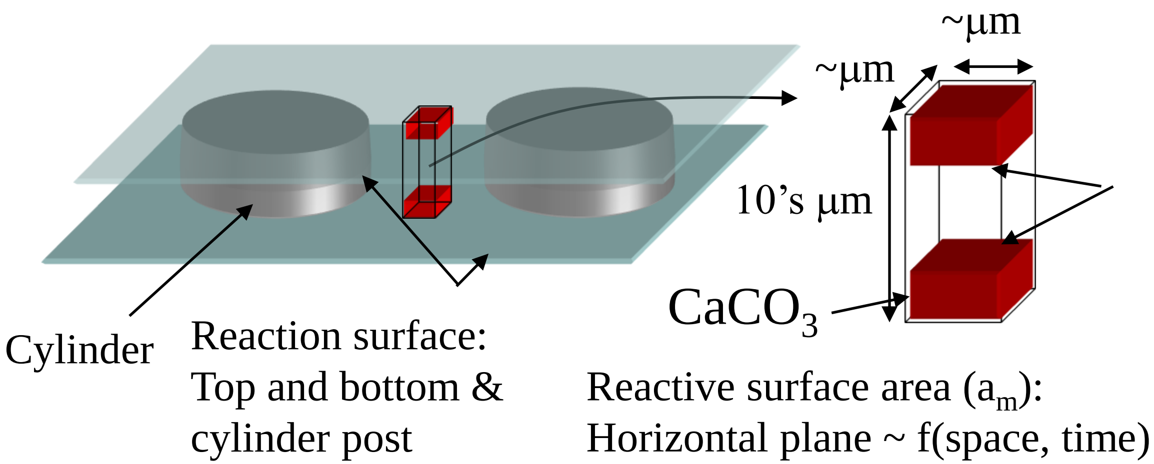

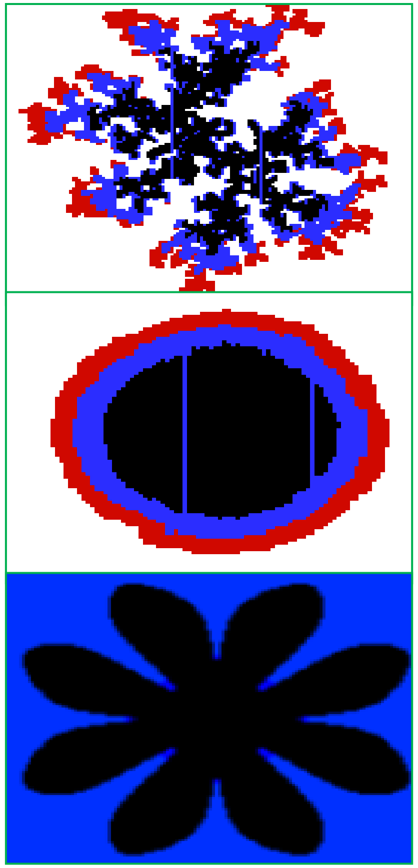

Effective diffusion coefficient = D_m * tortuosity (τ)

- $\tau(V_m) = (1 - V_m)^n$ where n ~ 0 to 3
- Diffusion is allowed until the grid cell is fully occupied by $CaCO_3$
- Crystal growth: cellular automata or other algorithms

Yoon et al. (WRR, 2012; RiMG2015)

Chen et al. (IJHMT, 2014)

- Motivations
- Reactive transport processes
- **Validation of pore scale transport models**
- Precipitation and dissolution cases
- Other applications
- Summary

Non reactive transport with tracer experiments

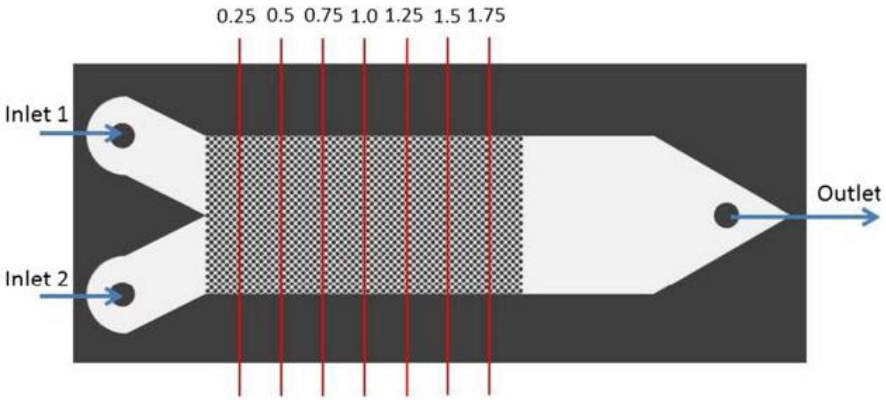

Experiment

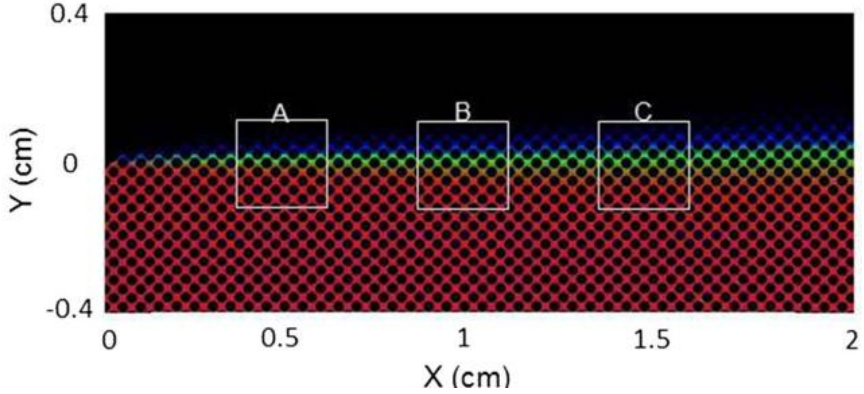

Pore scale transport modeling

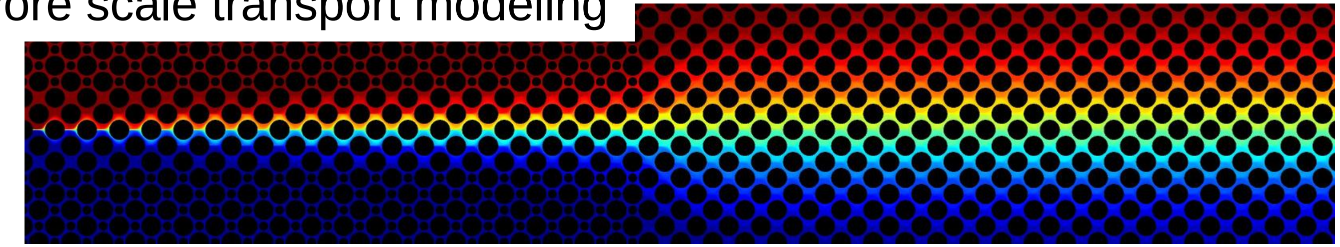

Four sets of nonreactive solute transport experiments in microfluidics

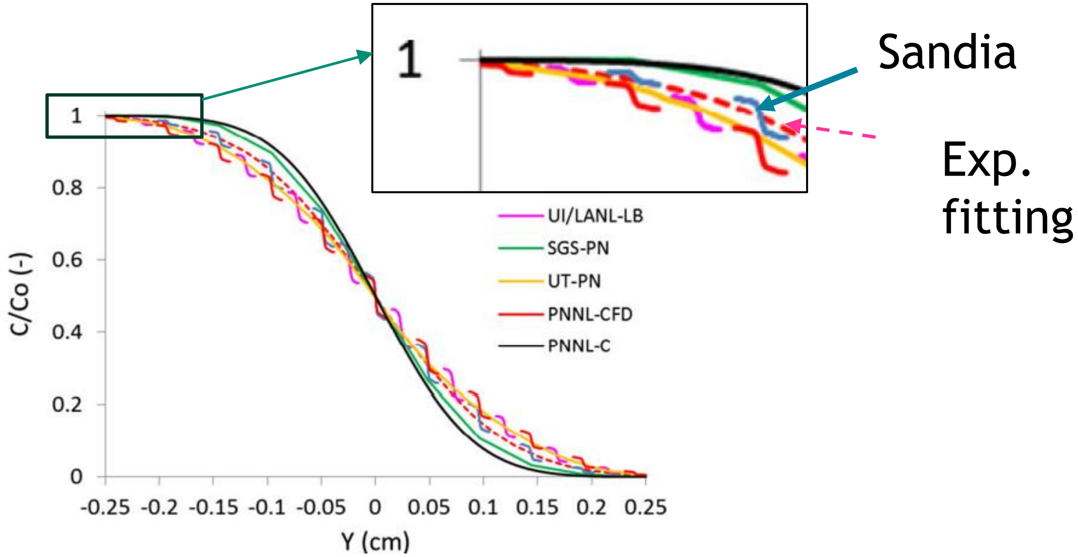

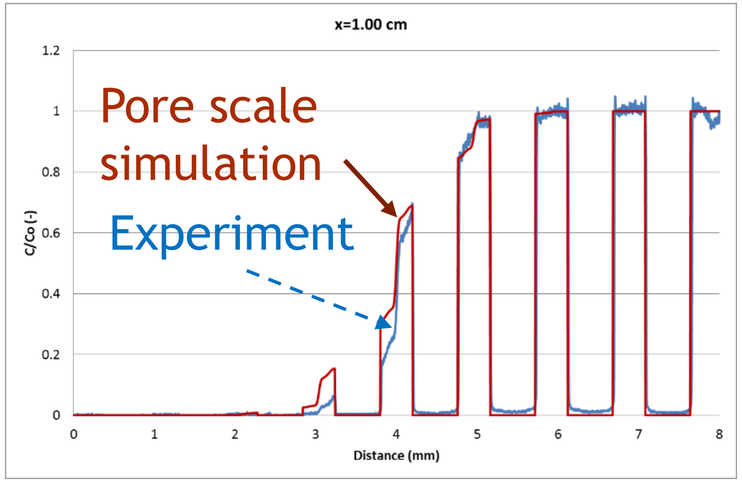

Quantitative comparison of experimental and numerical results

Oostrom et al. (Comput Geosci, 2016)

Transversely mixing induced reaction in a microfluidic

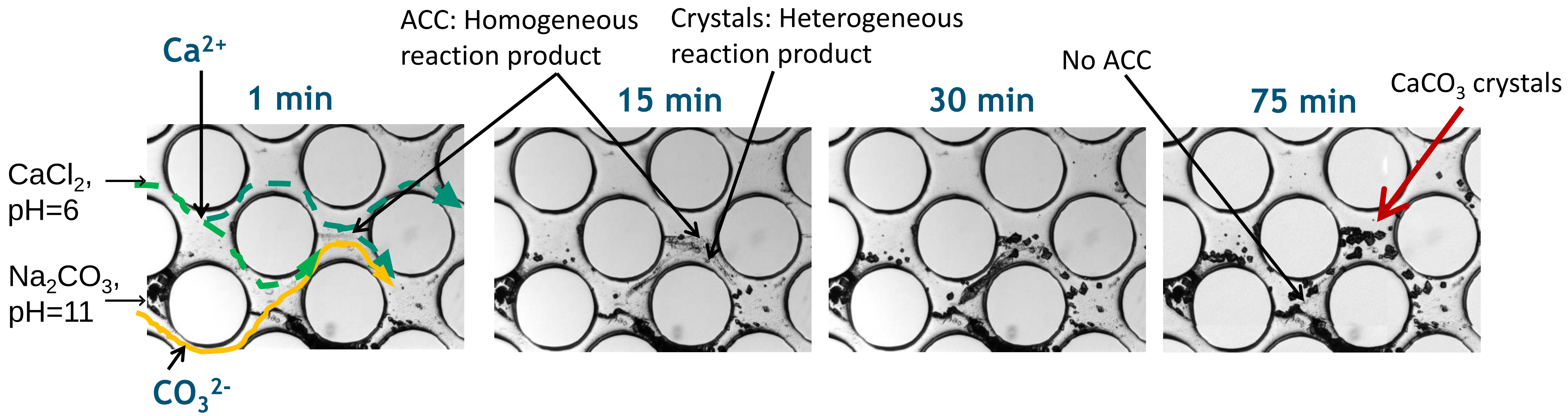

- Experimental observations:
  - ✓ Nanoparticles were optically observed, indicating amorphous calcium carbonate (ACC) formation. ➔ Initial ACC created $CaCO_3$ particles on microfluidic surfaces, creating favorable heterogeneous surface for $CaCO_3$ precipitation. Less structured particles become stable by transforming into more stable polymorphs

Simulated pH Distribution

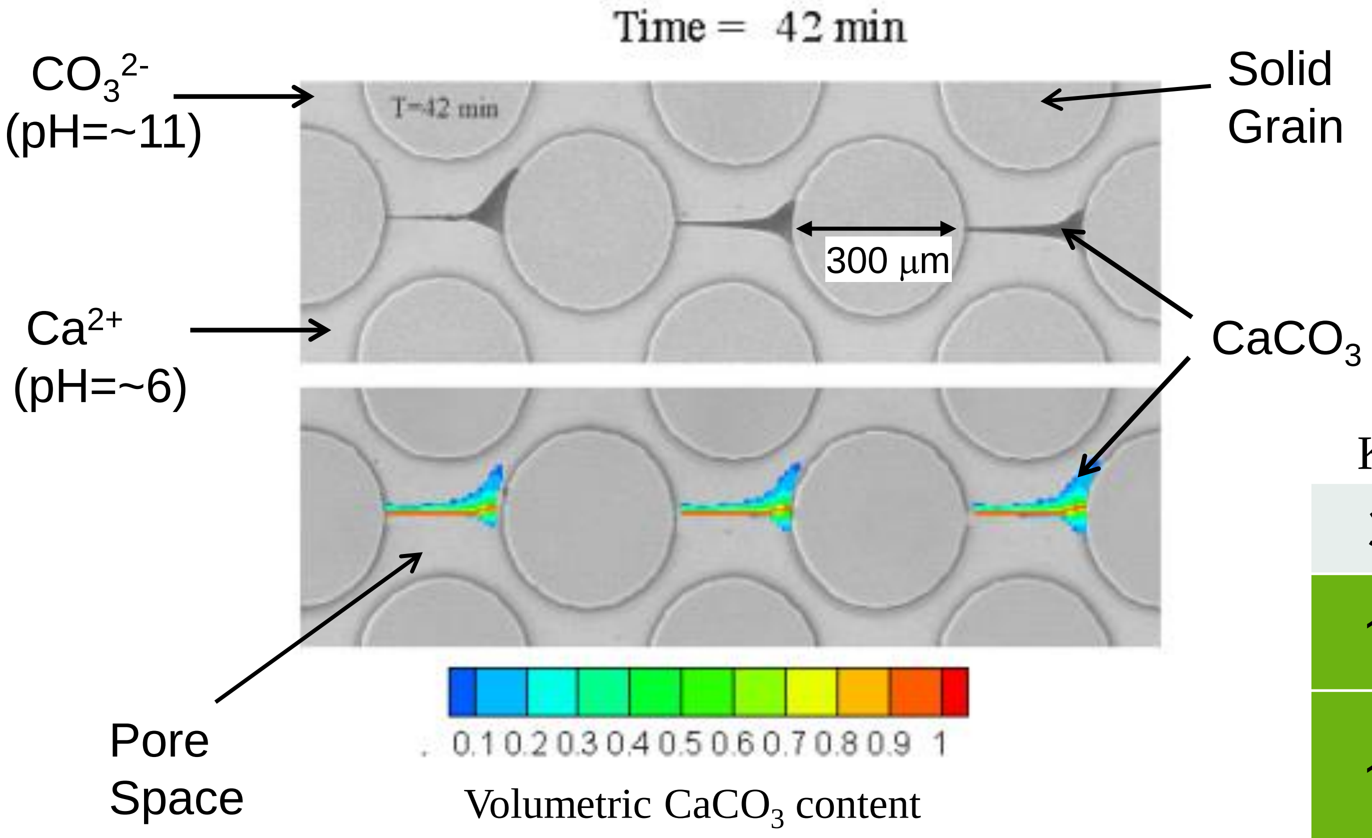

Simulated pH distribution (42min)

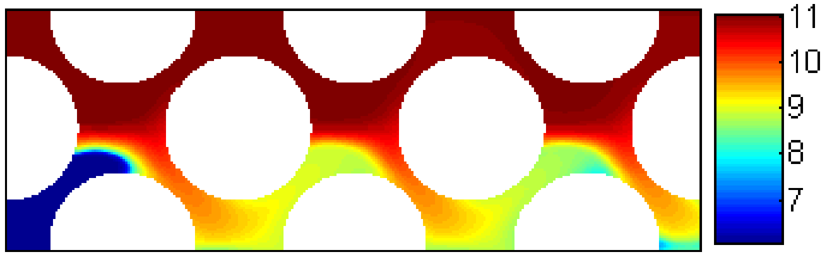

K_{sp} (Calcite)	K_{sp} (ACC)	
3.31E-09	5.58E-07	
1.27E+03	7.55E+00	$a_{CO_3^-}$ at pH of inlet solution (pH=11)
1.16E+02	6.86E-01	$a_{CO_3^-}$ at the mixing line (pH=9)

- Experimental observations:
  - ✓ $CaCO_3$ reaction products were only observed at a minimum concentration of ~6.5mM: IAP of Ca^{2+} and CO_3^{2-} needs to exceed K_{sp} of calcium carbonate (ACC) on non-favorable reaction surface (SiO_2) of the microfluidics

Yoon et al. (WRR, 2012)

Simulation results – Increasing reaction rate during dissolution by 300 (Case 5)

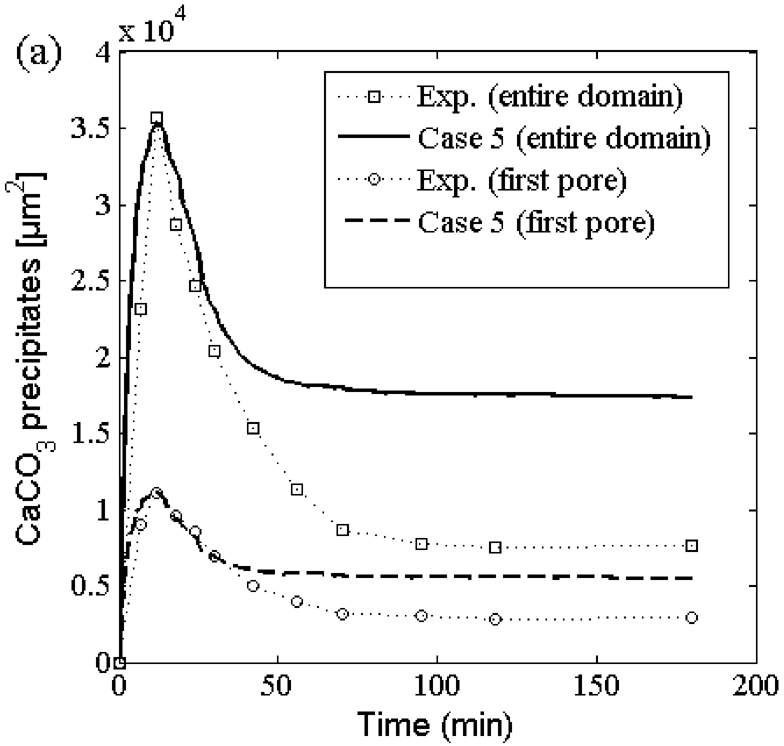

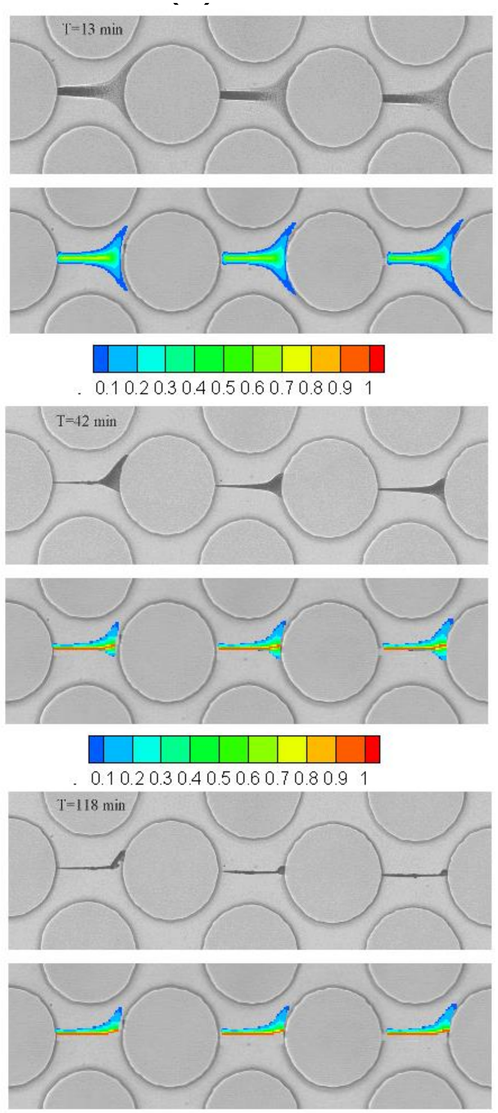

13 min

42 min

118 min

- Model results match thickness and area of precipitate until 30 min with a high dissolution rate (x300)
- Model predicts dissolution below the centerline well, but not above the centerline

Image process for quantitative analysis

- Image segmentation for identifying pixels of precipitates, reactive surface area, and reaction rates

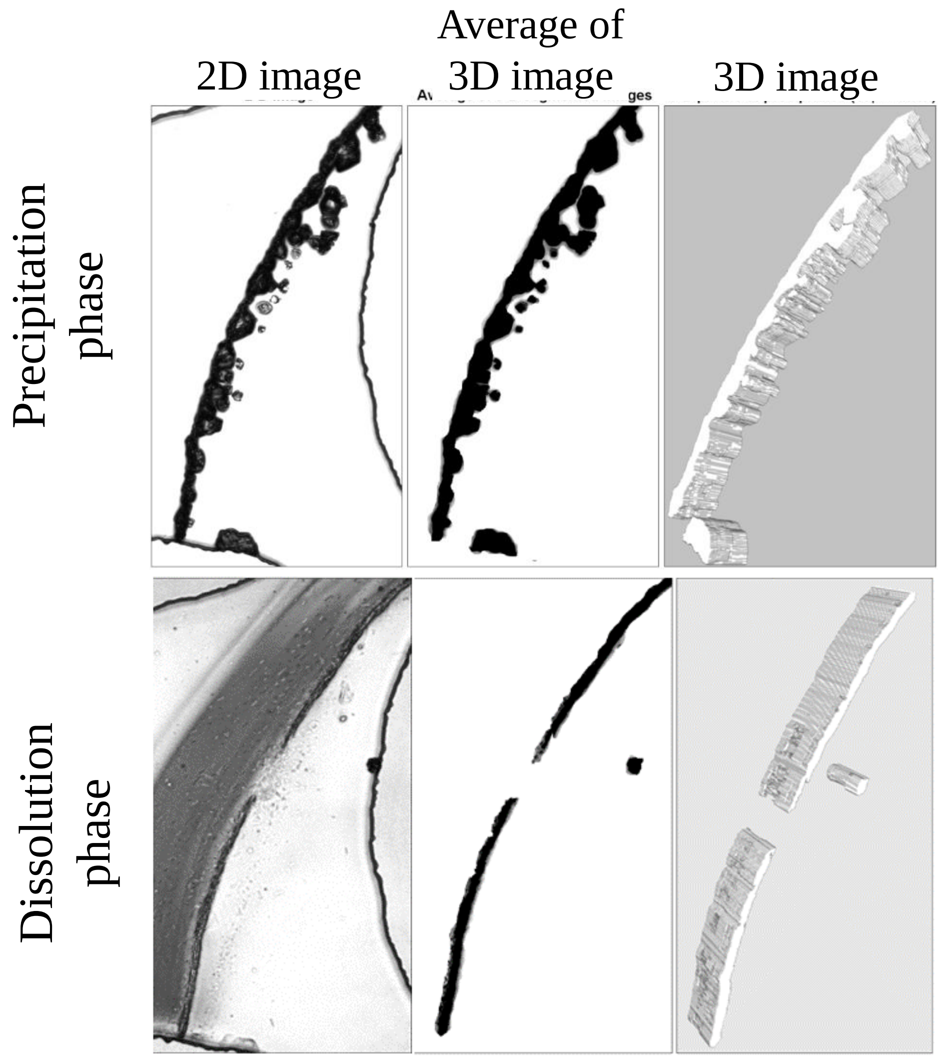

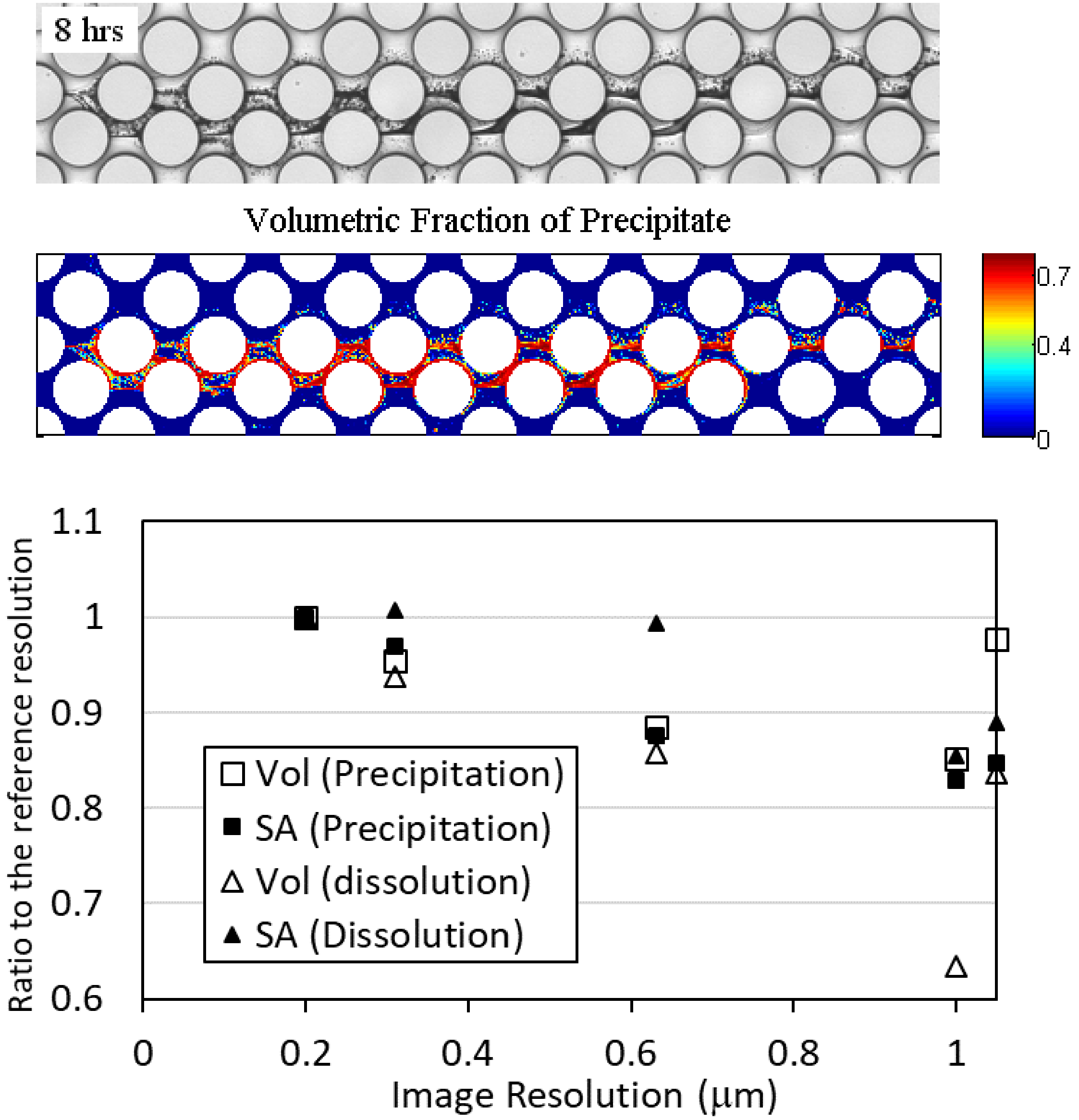

Yoon et al. (ES&T, 2019)

- Motivations
- Reactive transport processes
- Validation of pore scale transport models
- **Precipitation and dissolution cases**
- Other applications
- Summary

Large scale application for Crystal Geyser, Utah

- Observations along the surface exposure of the Grand Wash fault indicate alteration zones of 10-50 m width with spacing on the order of 100 m
- Locations of conduits controlled by fault-segment intersections and/or topography
- Sandstone permeability reduced by 3 to 4 orders of magnitude in alteration zones by carbonate cementation

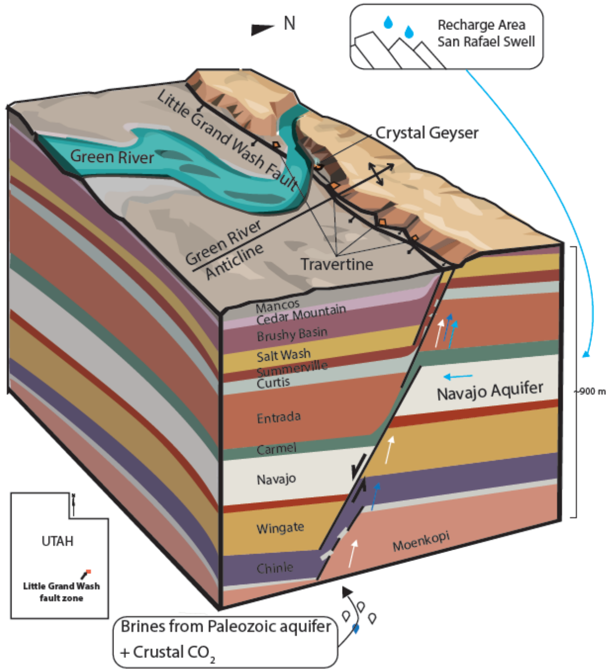

Altman et al. 2014

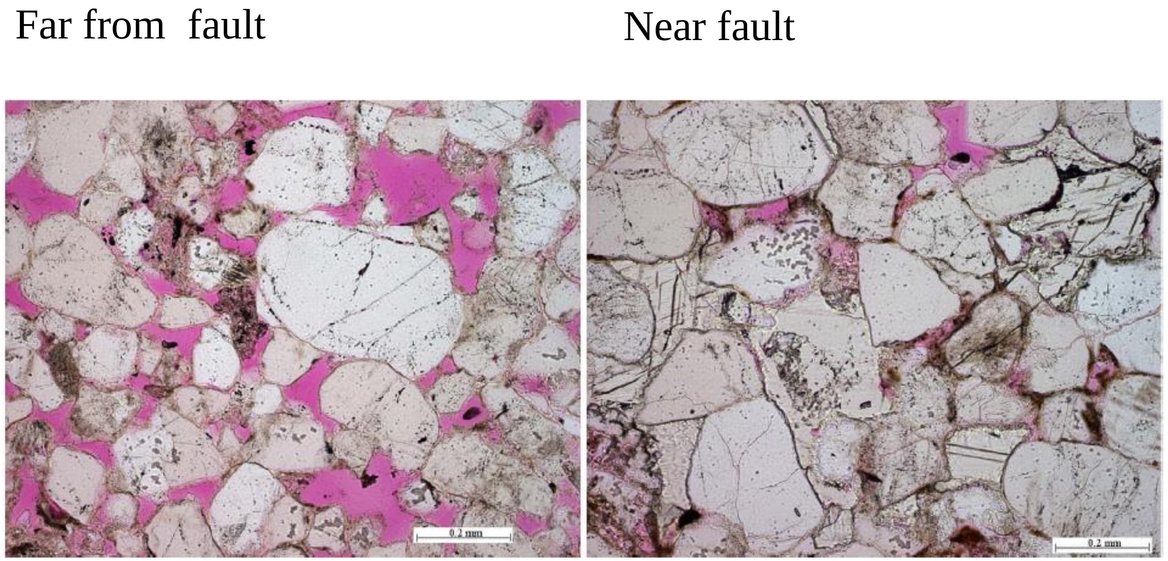

Yoon et al. JPSE 2017

Upscaled permeability and porosity relationships

Pore scale reactive transport modeling

Upscaled relationship

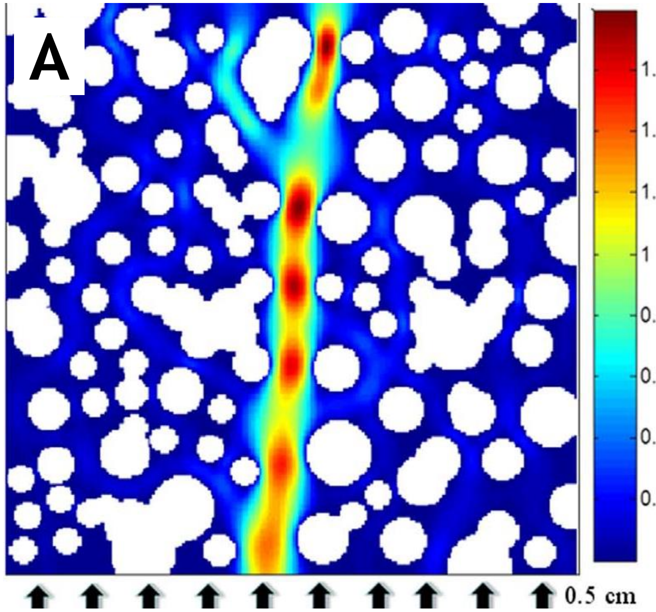

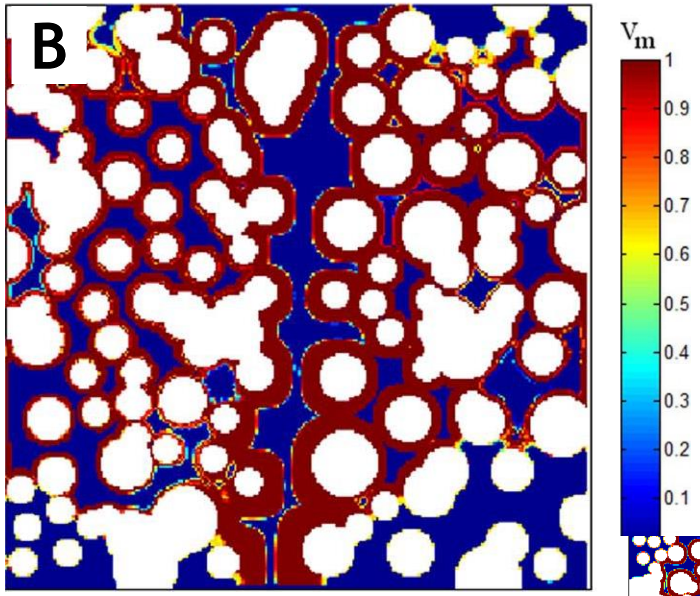

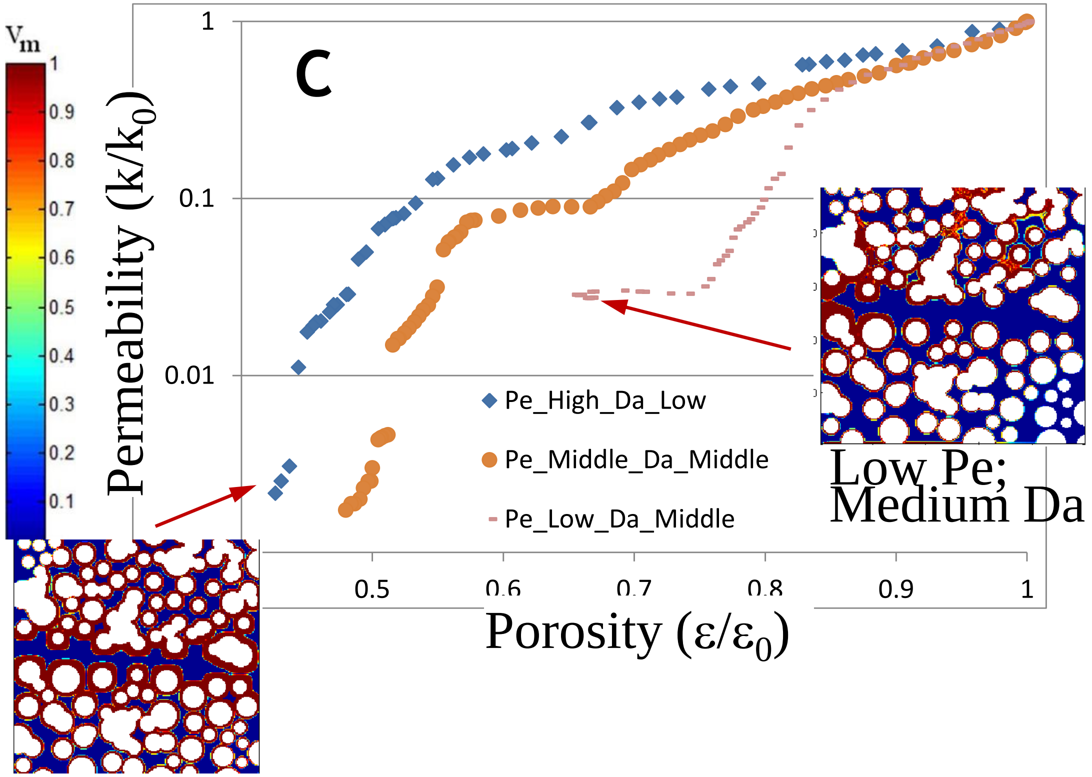

High Pe;
Low Da

Pe (uL/D) = 0.08, 0.8, 8

Da ($kL/(K_{sp}^{0.5} \times D)$) = 0.002, 0.02, 0.1

(A) Velocity profile in a porous medium with a high permeable conduit surrounded by grains (white), (b) a volumetric fraction of calcium carbonate precipitants, and (C) permeability-porosity relationships during cementation for various Pe and Da numbers (Yoon et al., 2017).

Yoon et al. JPSE 2017

Heterogeneous vs. homogeneous reactive surfaces

Inlet concentrations

$[Ca^{2+}]_T = [CO_3^{2-}]_T = 50mM$

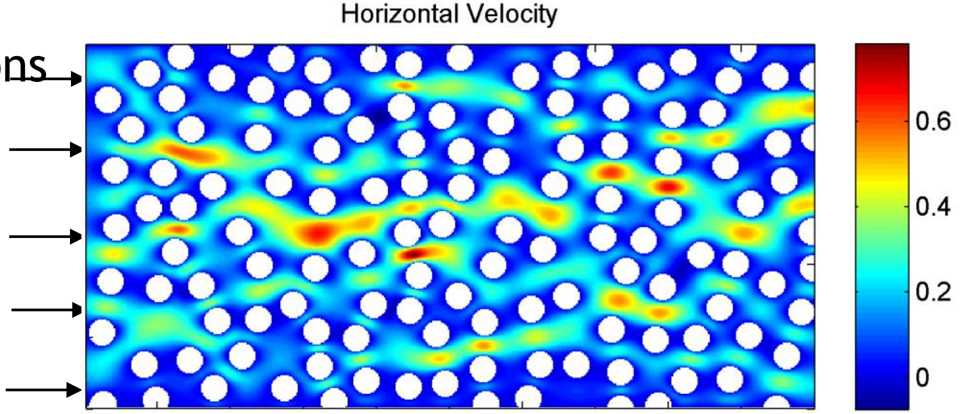

Velocity profile (pressure gradient)

Non-reactive grain

Reactive calcite

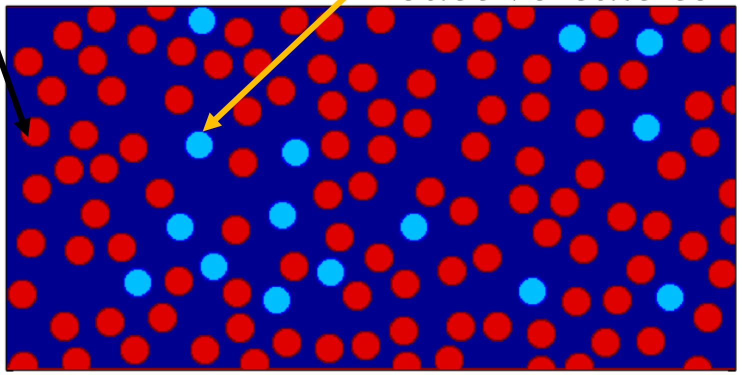

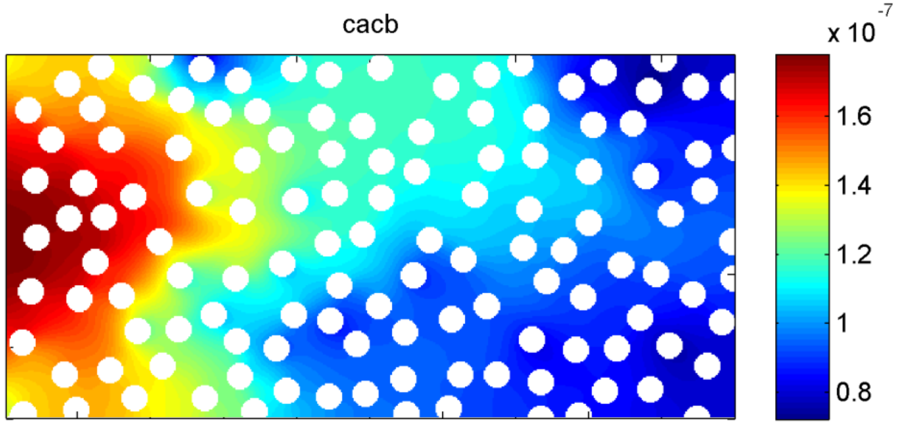

$\{Ca^{2+}\} \times \{CO_3^{2-}\}$ Concentrations

All reactive grains

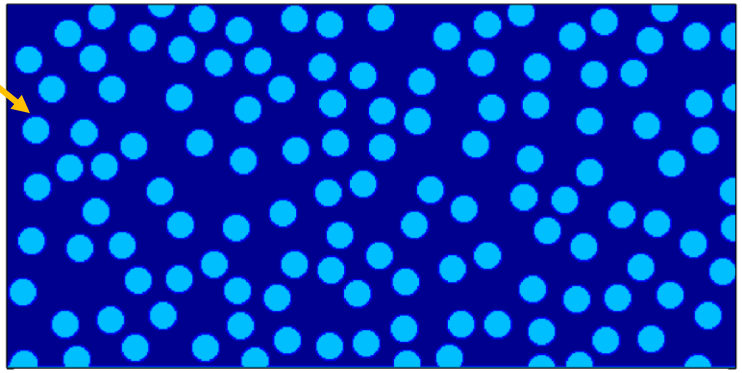

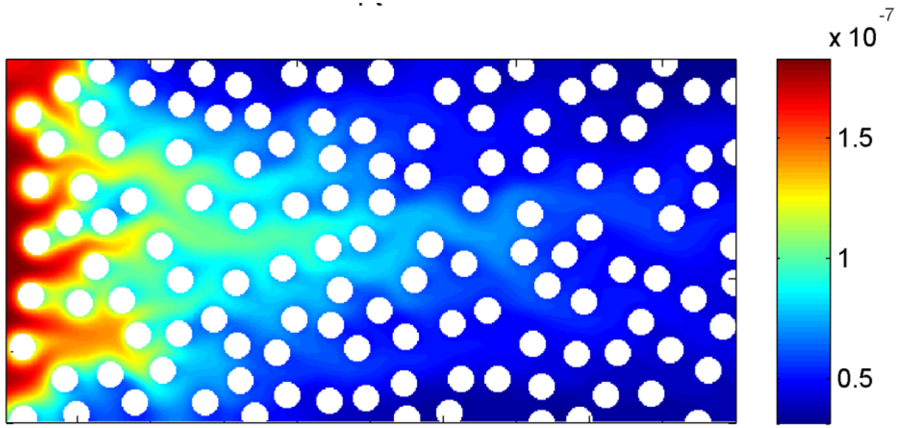

$\{Ca^{2+}\} \times \{CO_3^{2-}\}$ Concentrations

Heterogeneous vs. homogeneous reactive surfaces

Inlet concentrations
$[Ca^{2+}]_T = [CO_3^{2-}]_T = 50mM$

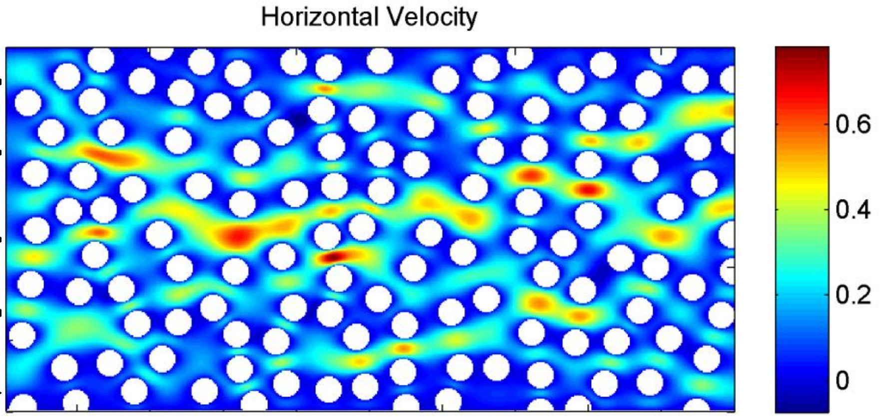

Velocity profile (pressure gradient)

Non-reactive grain

Reactive calcite

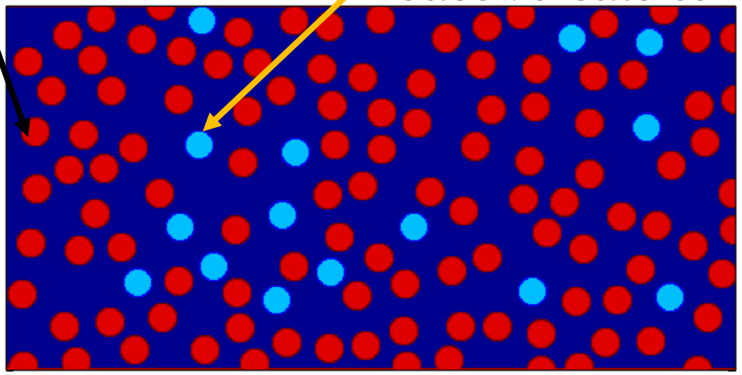

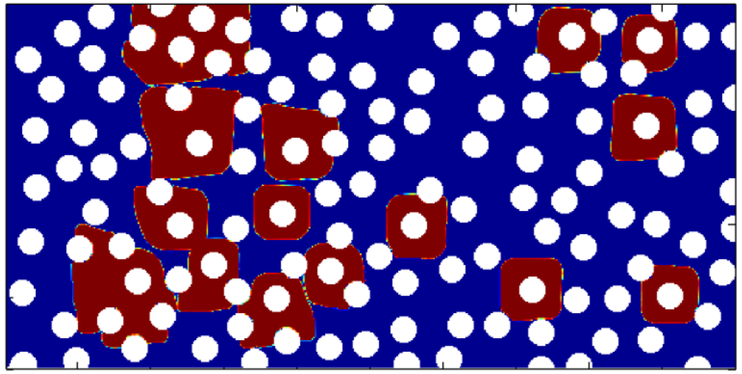

Concretion from reactive grains

All reactive grains

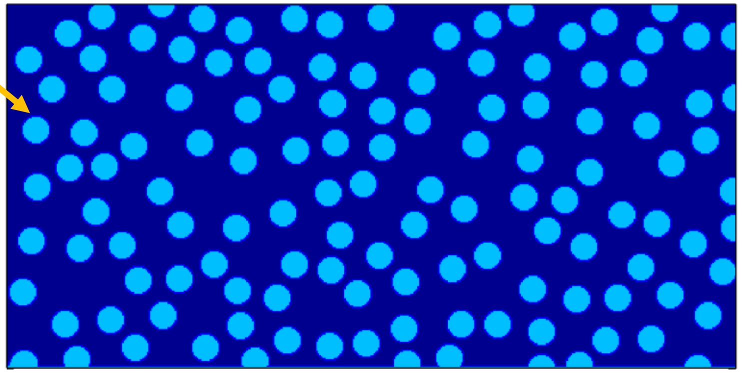

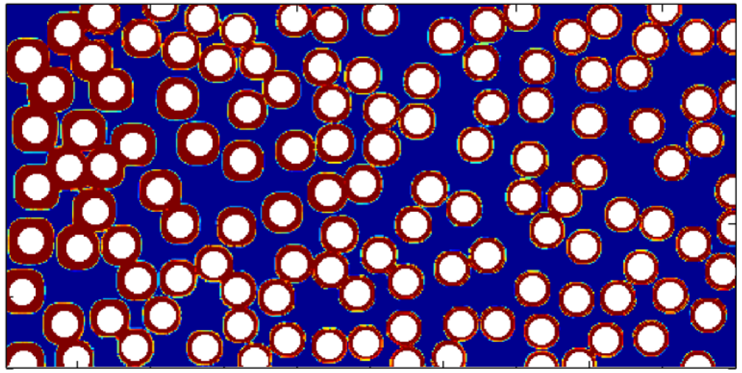

Concretion from all reactive grains

Different Pe & grain size distribution

All grains are reactive

Varying grain sizes at same locations

Moderate Pe & moderate Da

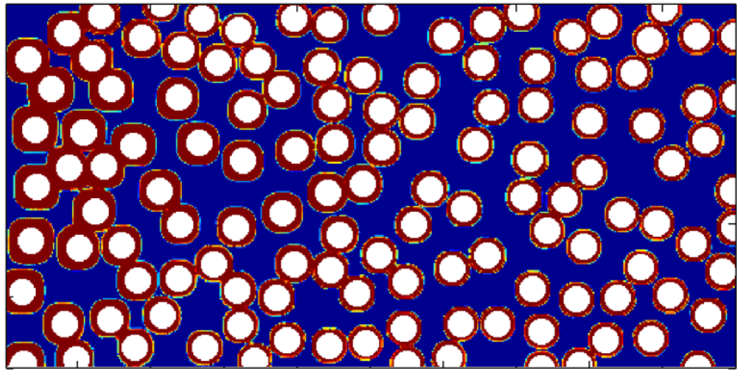

High Pe & moderate Da

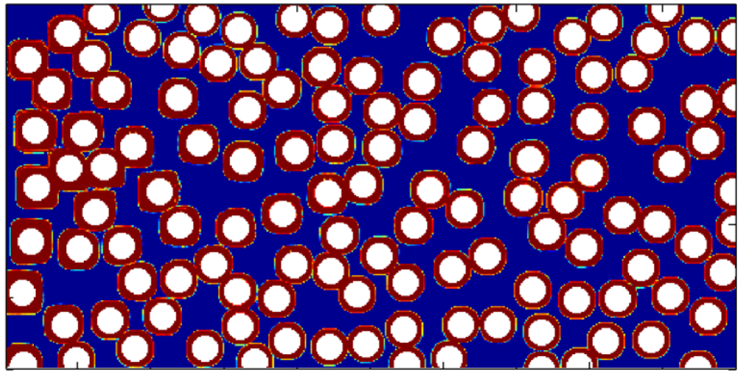

High Pe & moderate Da

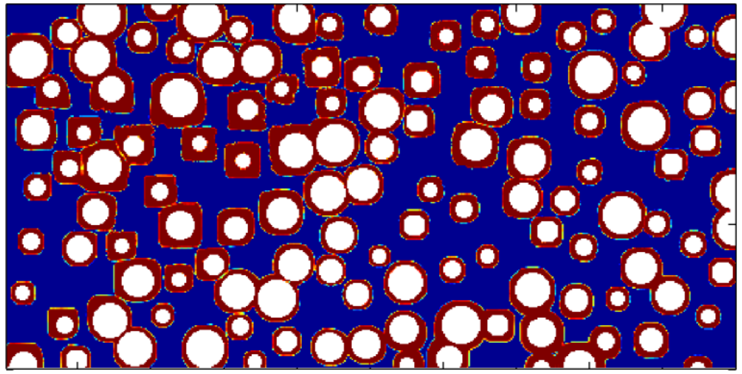

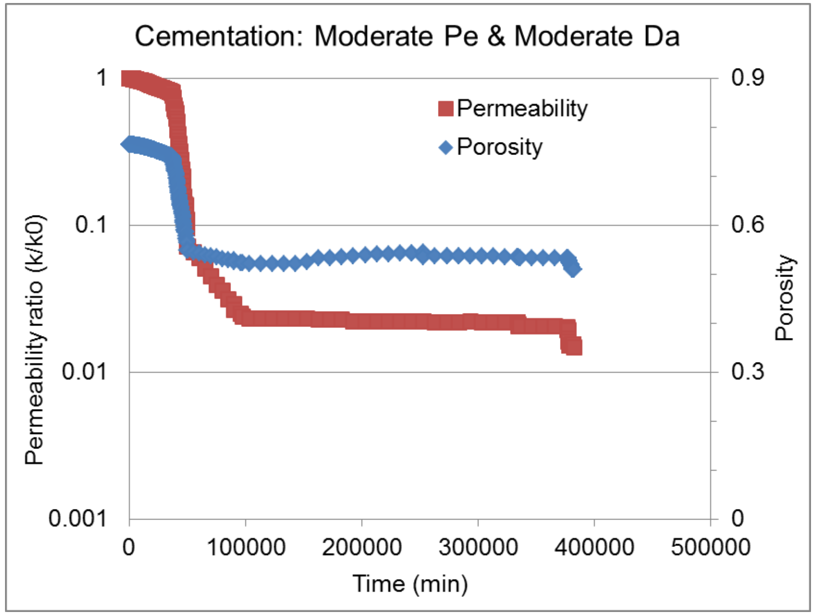

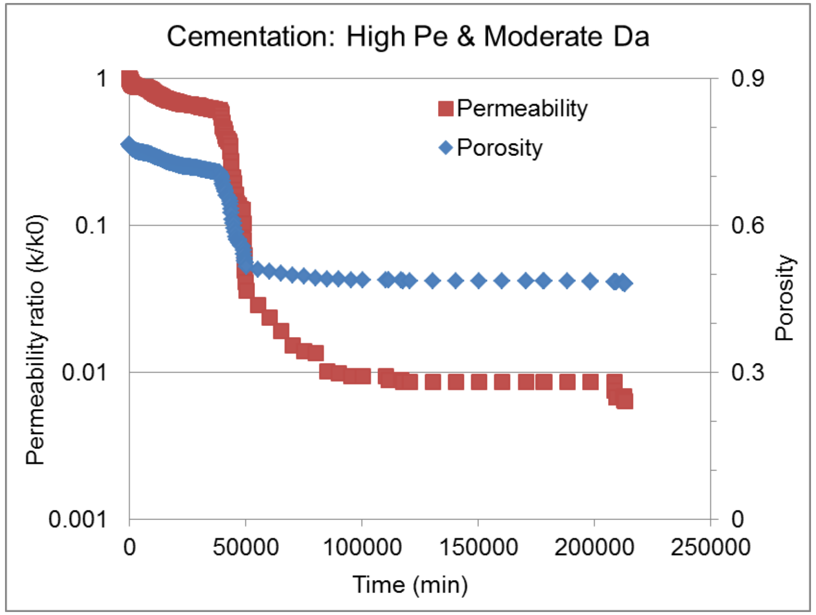

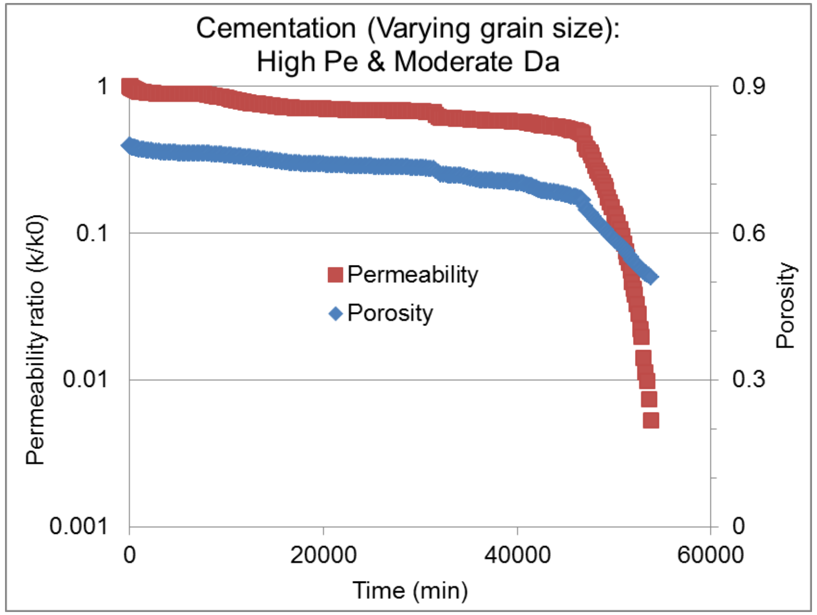

Permeability and porosity changes with cementation (time)

Different Pe & grain size distribution

All grains are reactive
Moderate Pe & moderate Da

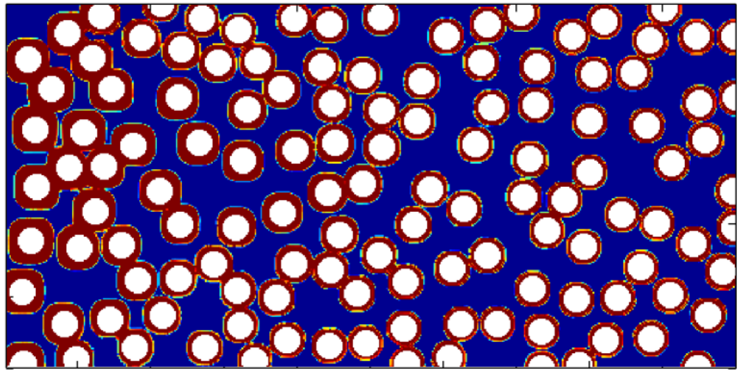

A fraction of grains are reactive
Moderate Pe & moderate Da

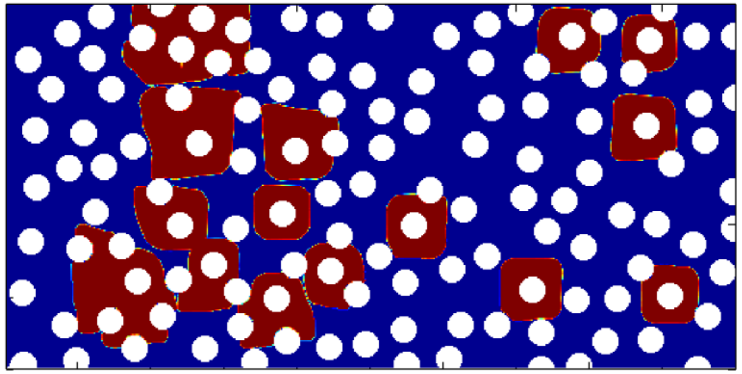

All grains are reactive
Varying grain sizes at same locations
High Pe & moderate Da

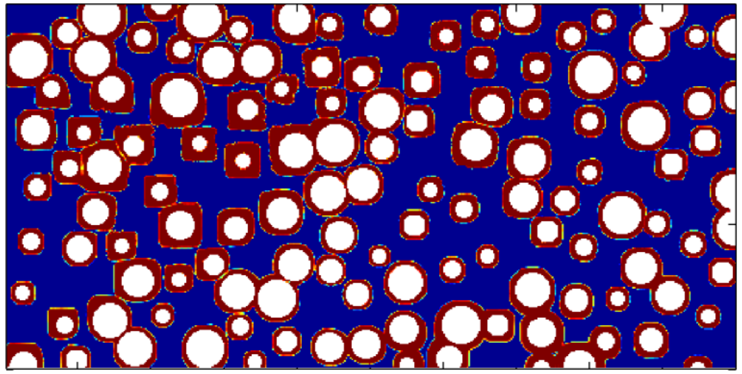

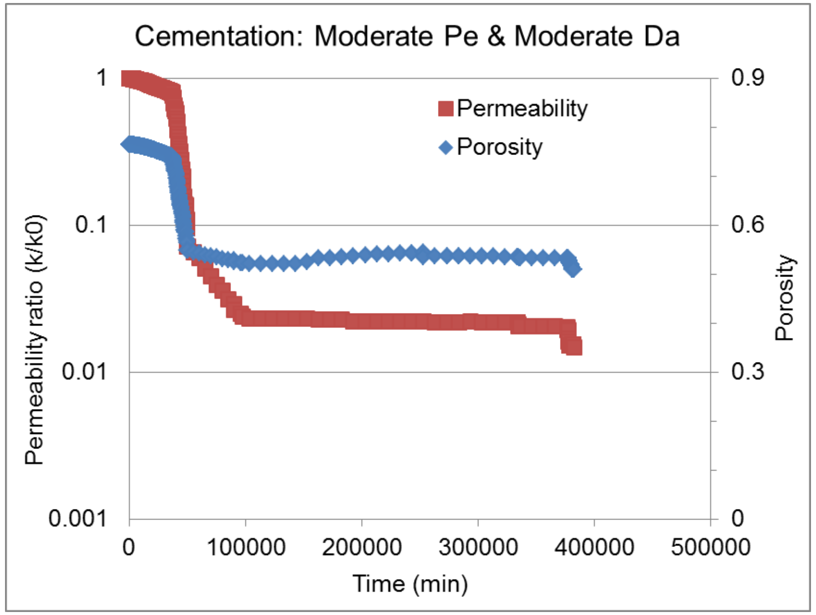

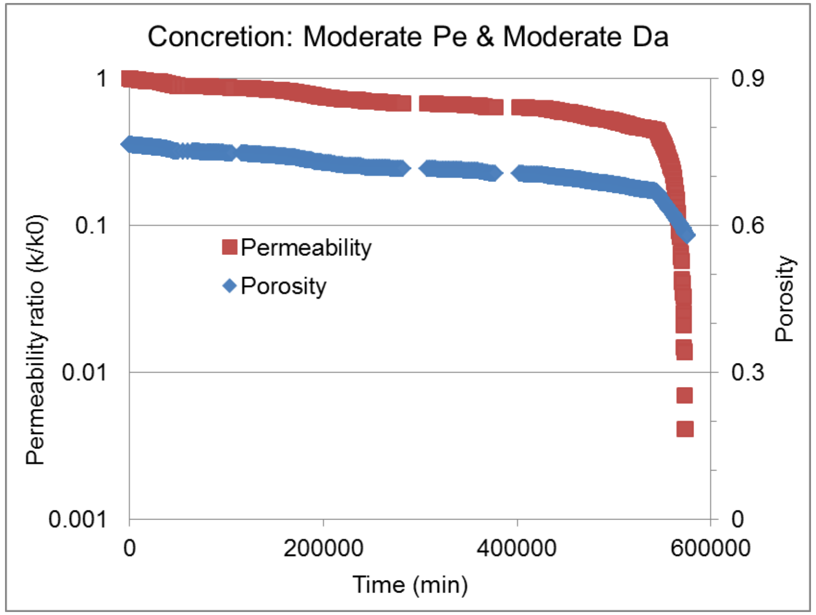

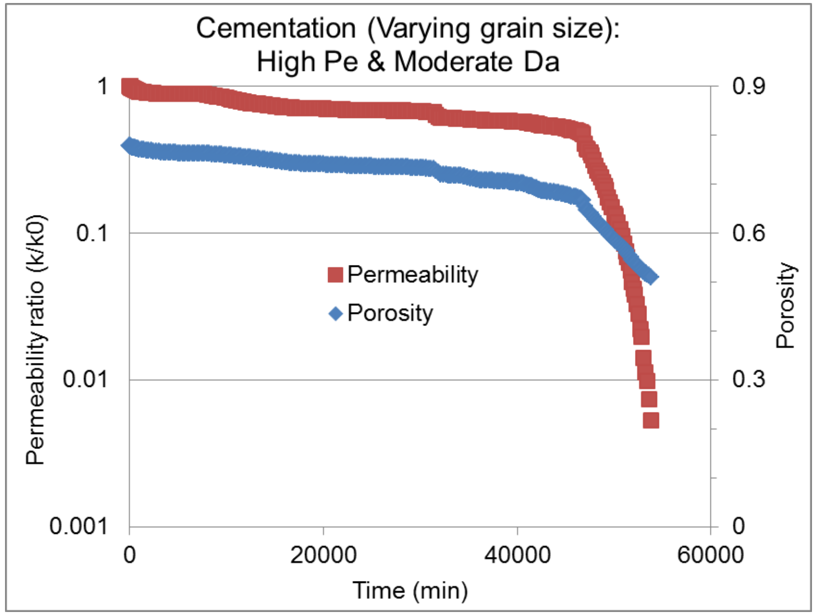

Permeability and porosity changes with cementation (time)

- Motivations
- Reactive transport processes
- Validation of pore scale transport models
- Precipitation and dissolution cases
- **Other applications**
- **Summary**

Reactive Transport: Biogeochemical reactions

Adaptation of *Delftia acidovorans* for degradation of 2,4-dichlorophenoxy-acetate

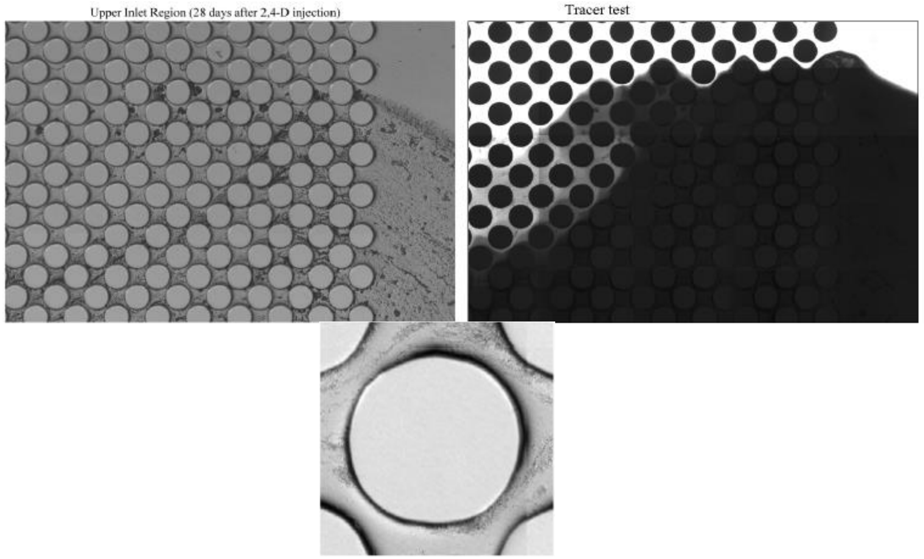

Bacteria adaptation experiments in flowing conditions (~ 1 year period)

Yoon et al. (Biodeg., 2014)

$CaCO_3$ biomineralization with denitrification (*Pseudomonas stutzeri*)

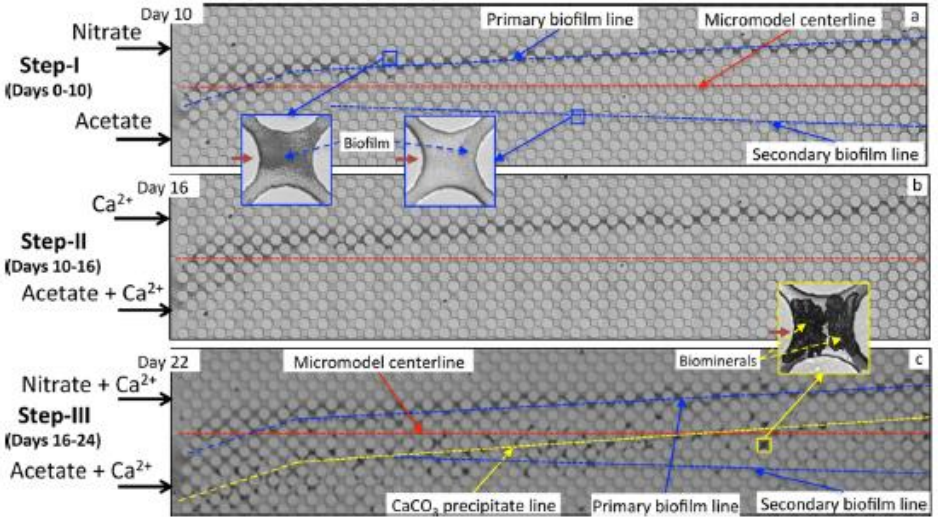

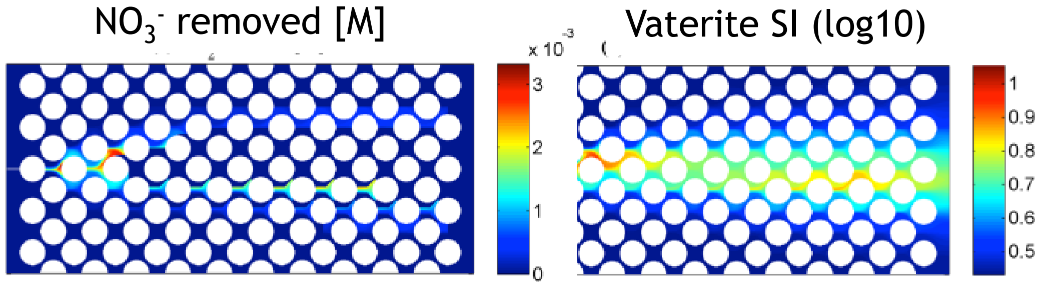

Singh, Yoon et al. (ES&T, 2015)

Microfluidic fabrication and Multiphase flow experiments

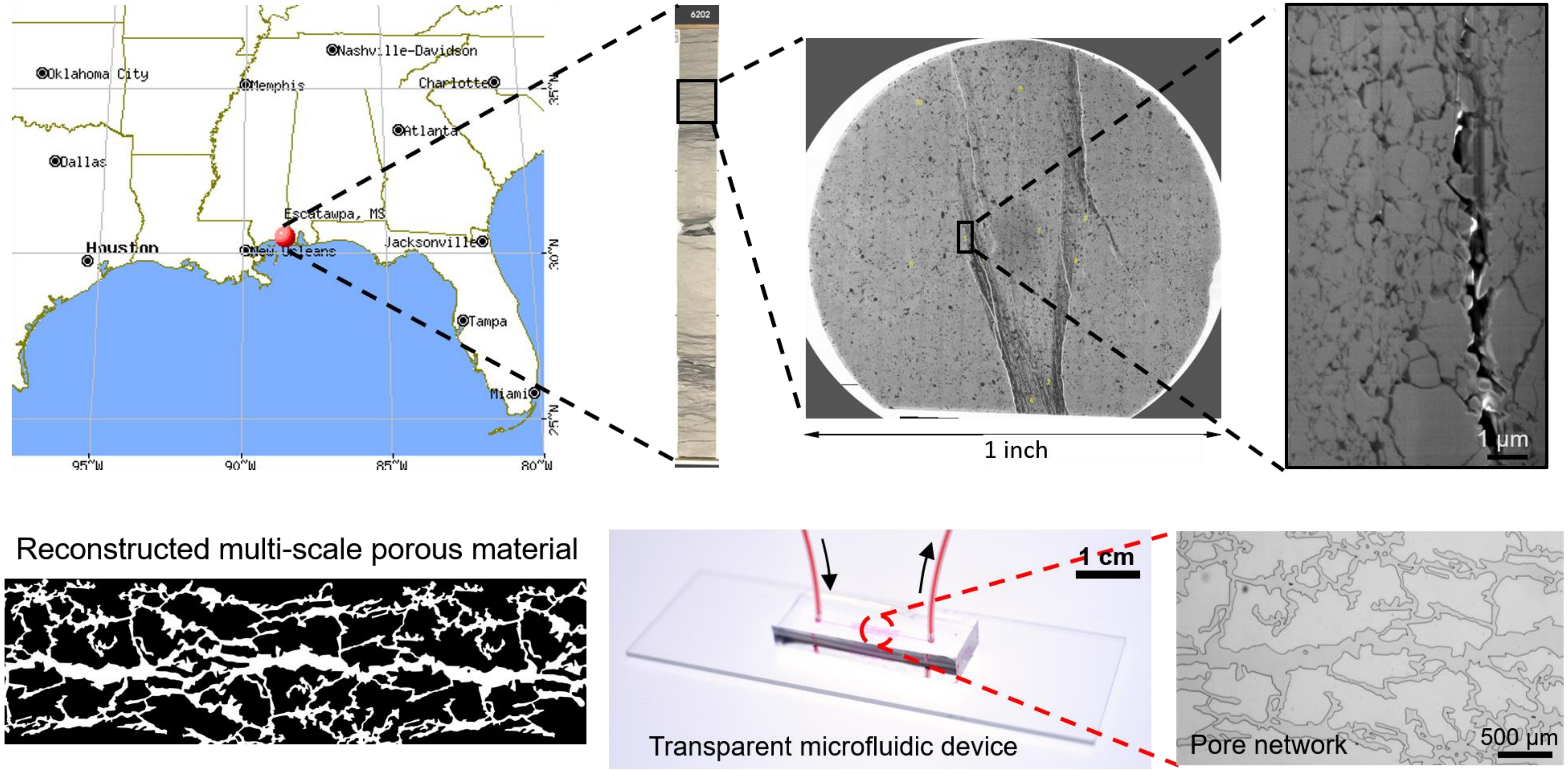

Park et al. (E&F, 2021)

Microfluidic fabrication and Multiphase flow experiments

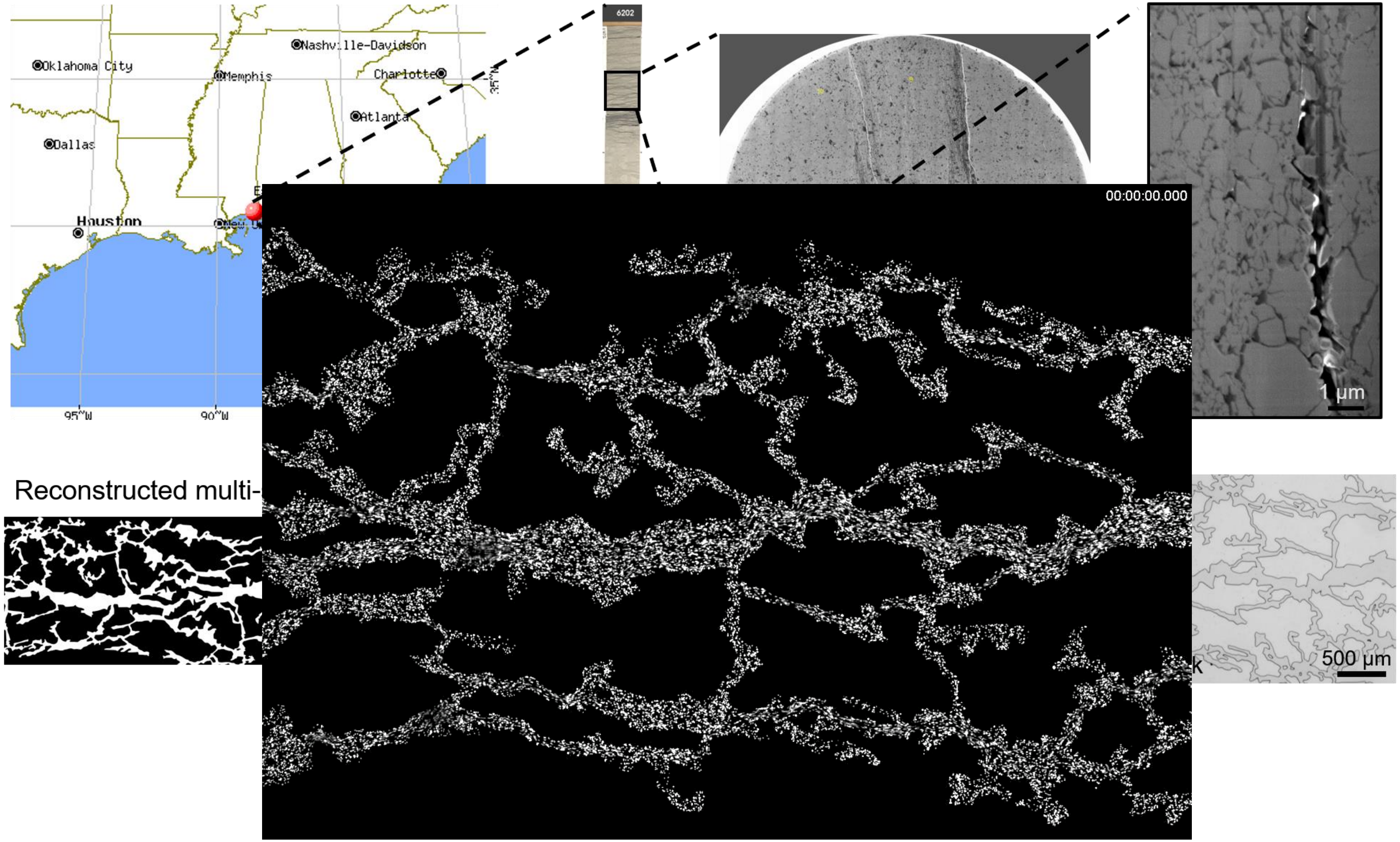

Oil emulsion flow

Park et al. (E&F, 2021)

Chemo-mechanical Processes in Nano-porous Chalk

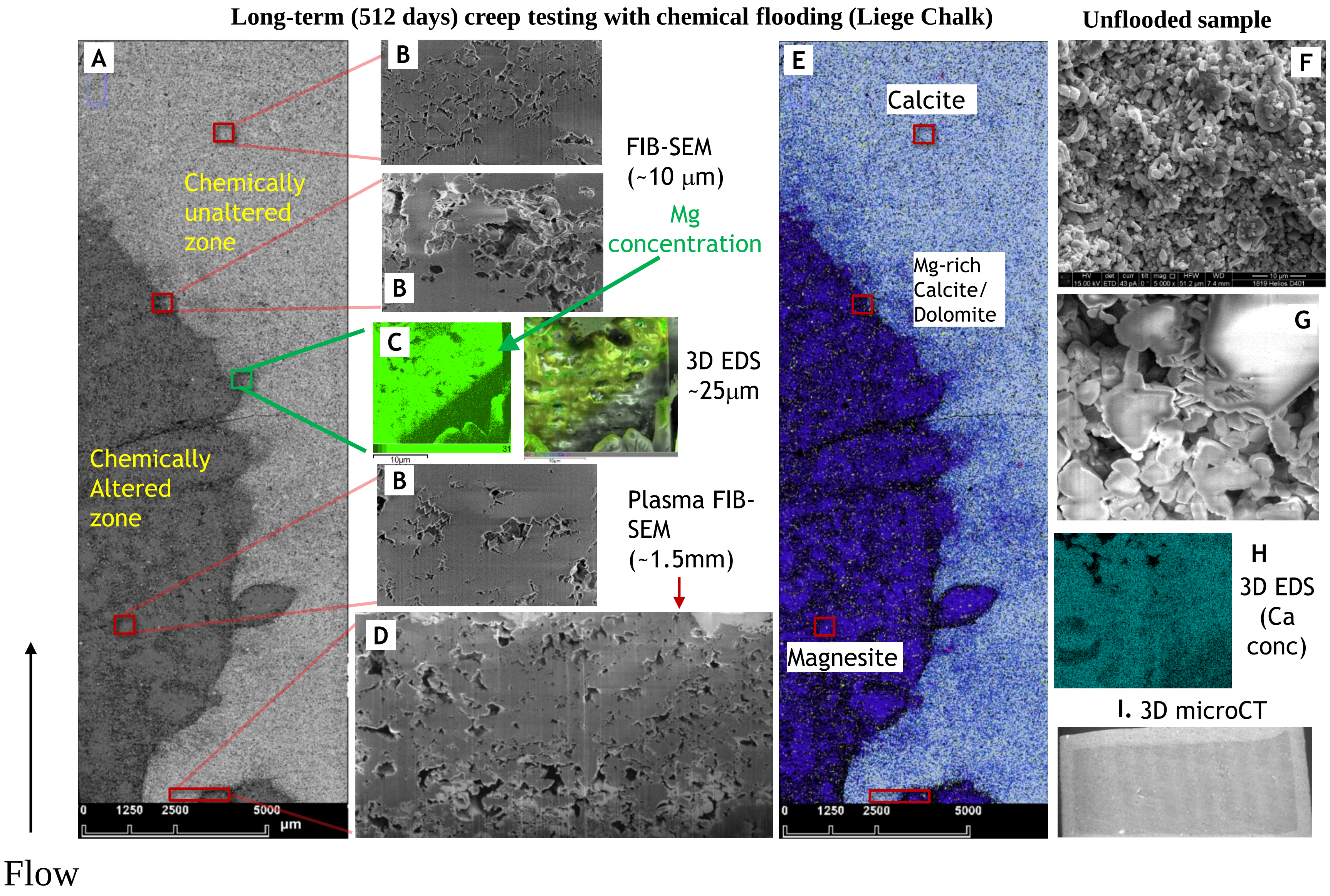

Samples from Nermoen et al., (JGR,2015)

Yoon et al. (In prep)

Summary

- Pore scale reactive transport enabled us to improve fundamental understanding of physico-chemical processes of $CaCO_3$ precipitation and dissolution
- Detailed investigation of reaction processes under more complex conditions (e.g., EGS) can be utilized to derive quantitative results of reactive transport processes
- Integration of experimental, numerical, and detailed data analysis will lead us to apply the reactive transport in microfluidic for many other problems
- An adaptive strategy to couple pore- and continuum scale using machine/deep learning methods will be tested against cement precipitation patterns

Thank you!!!
Questions?

Upscaled permeability and porosity relationships

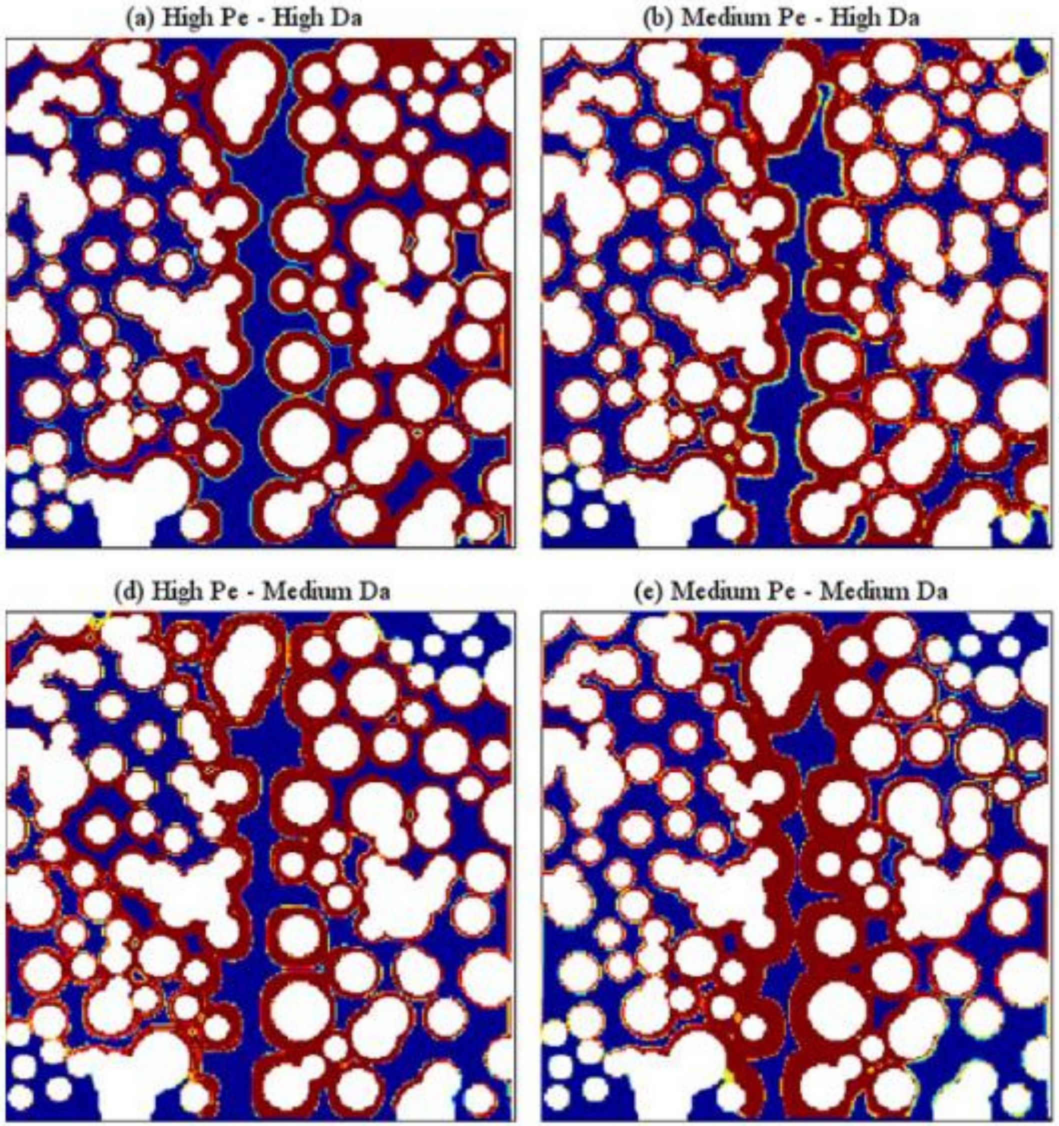

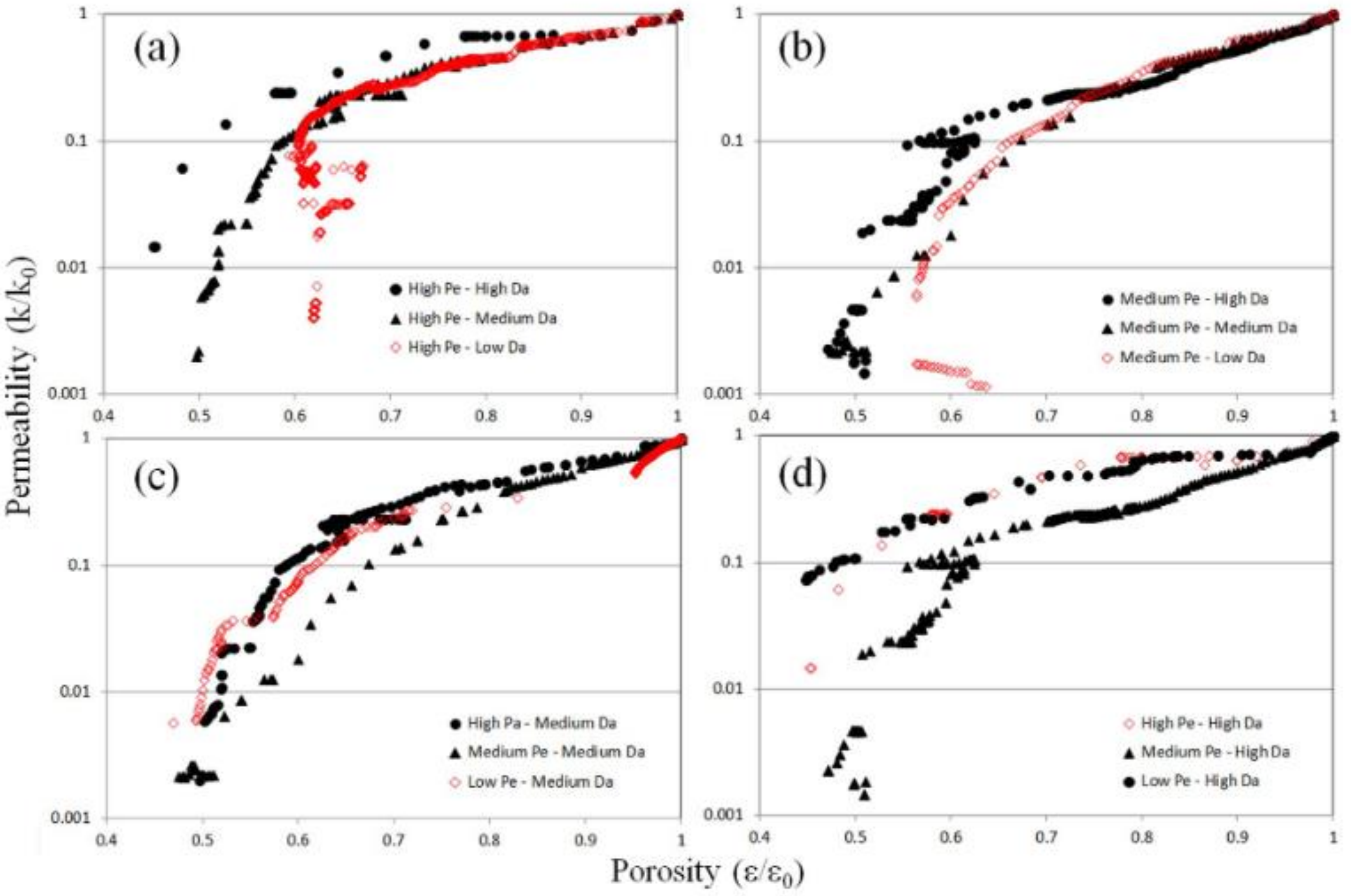

Fig. 5. Permeability-porosity relationships during cementation for various Pe and Da numbers.